Chemical Geology 668 (2024) 122327

Contents lists available at ScienceDirect

Chemical Geology

journal homepage: www.elsevier.com/locate/chemgeo

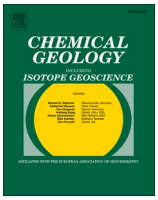

# New insights on Late Pliensbachian-Early Toarcian seawater chemistry based on belemnite rostra element content

Ricardo L. Silva [a,*], Juan J. Gómez [b], Ángela Fraguas [c]

[a] Department of Earth Sciences and BETY Lab - PaleoSed+ Research Group, Clayton H. Riddell Faculty of Environment, Earth, Resources University of Manitoba, 230 Wallace Building, 125 Dysart Road, Winnipeg, Manitoba R3T 2N2, Canada
[b] Departamento de Geodinámica, Estratigrafía y Paleontología, Facultad de Ciencias Geológicas, Universidad Complutense de Madrid e IGEO (CSIC), Jose Antonio Novais 12, 28040 Madrid, Spain
[c] Departamento de Biología y Geología, Física y Química Inorgánica y Grupo de Investigación en Dinámica de la Tierra y Evolución del Paisaje (Dynamical), ESCET, Universidad Rey Juan Carlos, 28933 Móstoles, Spain

ARTICLE INFO

Editor: Vasileios Mavromatis

*Keywords:*
Elemental geochemistry
Belemnites
Calcareous nannofossils
Paleo-oceanography
Early Jurassic
Spain

ABSTRACT

Belemnites were a type of cephalopod abundant in the Jurassic and Cretaceous, whose fossils have been extensively used for paleo-oceanographic studies. For this study, we analyzed 69 elements by Inductively Coupled Plasma-Sector Field Mass Spectrometry (ICP-SFMS) in 15 belemnite rostra from the West Rodiles section in the Asturian Basin, Northern Spain. We aim to determine if belemnite rostra carbonate chemistry reflects changes in seawater chemistry during the Late Pliensbachian–Early Toarcian time interval and examine how belemnites can be used to trace known drivers of the Early Toarcian Oceanic Anoxic Event (T-OAE) and associated oceanographic processes.

Discarding drastic intra-species effects and assuming a similar influence of growth rates, diet, and other physiological processes for all analyzed belemnite specimens and taking into consideration the sizeable analytical uncertainty, we assess if determined belemnite rostra element chemistry reflects broad and relative changes in paleo-seawater chemistry. Many determined elements are present in only ppb amounts, and their interpretation is uncertain. We found that Mg, Mn, and P increase in the interval chronocorrelative to the T-OAE. This is interpreted to have resulted from an increase in these elements' inventory in seawater due to an increase in continental weathering and fluvial runoff associated with this global event. Iron, K, and Na contents decrease upwards in the section, potentially indicating that these elements became limited and likely hampered oceanic productivity. Our study also found a correspondence between a change in the behaviour of several elements, warming, the T-OAE negative CIE, and a reduction in the diversity and size of both calcareous nannofossils and belemnites in the study area.

## 1. Introduction

The Late Pliensbachian (188.0–184.2 Ma) and Early Toarcian (184.2–181.2 Ma) are times of large swings in global climate (Hesselbo et al., 2020); the latest Pliensbachian saw global cooling, whereas the Early Toarcian was a time of super-warming, or hyperthermal (De Baets et al., 2021; Dera et al., 2009; Gómez et al., 2008; Gómez and Arias, 2010; Korte and Hesselbo, 2011; McArthur et al., 2000; Price, 1999; Rita et al., 2019; Rosales et al., 2004a; Ruebsam et al., 2020a,b; Ruebsam et al., 2019; Ruhl et al., 2016; Silva et al., 2021b; Silva and Duarte, 2015; Storm et al., 2020; Suan et al., 2010; Ullmann et al., 2020; Ullmann et al., 2014; Wignall et al., 2005).

Warming and significant perturbations to the Late Pliensbachian and Early Toarcian global carbon cycle have been linked to changes in global plate tectonic processes. It was recently hypothesized that changes in plate movement direction and reduction in local plate velocities led to thermal erosion of the African cratonic lithosphere by a deep mantle plume, resulting in the emplacement of the Karoo and Ferrar Large Igneous Province (LIP) (Ruhl et al., 2022). The Karoo and Ferrar LIP is postulated to have resulted in the release of isotopically light ($^{13}C$-depleted) volcanogenic $CO_2$ (Pálfy and Smith, 2000) and thermogenic methane ($CH_4$) from sill intrusions into Gondwanan coals (McElwain et al., 2005). It is thought that its global environmental effects were compounded by the release of biogenic methane from the dissociation of

* Corresponding author.
*E-mail addresses:* ricardo.silva@umanitoba.ca (R.L. Silva), angela.fraguas@urjc.es (Á. Fraguas).

https://doi.org/10.1016/j.chemgeo.2024.122327
Received 29 March 2024; Received in revised form 7 August 2024; Accepted 9 August 2024
Available online 10 August 2024

subseafloor clathrates (Hesselbo et al., 2000), terrestrial environments (Them et al., 2017), and labile cryospheric reservoirs (Krencker et al., 2019; Ruebsam et al., 2019; Silva and Duarte, 2015). Contemporaneous global perturbations to the global carbon cycle are expressed as positive and negative carbon isotope excursions (CIE) recorded in carbonates and organic matter, i.e., the Early Toarcian Oceanic Anoxic Event (T-OAE, Jenkyns, 1988), postulated based on globally distributed organic-rich facies. These facies characterize this time interval as a superregional organic matter preservation interval (OMPI, cf. Silva et al., 2021a) (Fig. S1).

The global environmental perturbations that characterized much of the early Toarcian (including, among other aspects, the T-OAE negative CIE) are sometimes collectively referred to as the Jenkyns Event (Müller et al., 2016; Reolid et al., 2020). This event is arguably associated with the largest carbon cycle perturbation of the Jurassic Period, reflected in the rock record by an up to ~7‰ negative shift in $\delta^{13}C$ of marine calcite and marine and terrestrial organic matter in the lower Toarcian Serpentinum ammonite chronozone (ACZ, e.g. Hesselbo et al., 2007; Jenkyns, 2010; Jenkyns et al., 2002). The T-OAE negative CIE is superimposed on a stratigraphically longer-lasting positive Toarcian trend, from the uppermost Spinatum ACZ (uppermost Pliensbachian) to the lower Bifrons ACZ (Toarcian) (e.g. Hesselbo et al., 2007; Jenkyns, 2010; Them et al., 2018; Xu et al., 2018; Ruebsam et al., 2020a,b) (Fig. S1).

Atmospheric $pCO_2$ is estimated to have at least tripled (McElwain et al., 2005) during this time interval, leading to an increase of about 4–10 °C in seawater temperatures, even at low- to mid-latitudes (Gómez and Goy, 2011), reduced ocean water pH with a decreased calcium carbonate saturation (Müller et al., 2020, but see Li et al., 2021), and a biocalcification crisis event in many different fossil groups, such as calcareous nannofossils (e.g., Clémence et al., 2014; Erba et al., 2019; Faucher et al., 2022; Fraguas et al., 2021; Fraguas et al., 2012; Fraguas and Young, 2011; Mattioli et al., 2009a; Mattioli et al., 2004; Peti and Thibault, 2017; Suan et al., 2008) and belemnites (Nätscher et al., 2021) Coeval environmental change on land resulted in a general enhancement of the hydrological cycle and silicate weathering and changes in vegetation and the prevalence of wildfires (Baker et al., 2017; Brazier et al., 2015; Jenkyns, 2010; Percival et al., 2016; Rodrigues et al., 2021; Rodrigues et al., 2020a; Rodrigues et al., 2020b; Rodrigues et al., 2019; Silva et al., 2021b; Slater et al., 2019; Them et al., 2019). An increase in seawater temperature led to a temperature-driven 2nd-order mass extinction that affected many groups of marine organisms in different basins around the world (Arias, 2009, Arias, 2006; Baeza-Carratalá et al., 2015, 2017; Caswell et al., 2009; Caswell and Coe, 2013; Caswell and Frid, 2017; Danise et al., 2015; De Baets et al., 2021; Dera et al., 2016; Fraguas et al., 2021, Fraguas et al., 2012; Fraguas and Young, 2011; Gómez and Arias, 2010; Little and Benton, 1995; Neige et al., 2021; Rita et al., 2021; Slater et al., 2019).

In detail, the response of several groups to the environmental drivers of the T-OAE was, generally, to decrease in size and diversity (e.g., Fraguas et al., 2021; Fraguas et al., 2012; Fraguas and Young, 2011; Martindale and Aberhan, 2017; Piazza et al., 2019; Ullmann et al., 2020). However, belemnite body size changes across the T-OAE are in contrast with several other organisms, and a general increase in median rostrum size is observed due to the appearance of new and larger taxa associated with a marked taxonomic turnover (De Baets et al., 2021). Also, the response of belemnite diversity to the environmental drivers of the T-OAE is regionally disparate; diversity (at a zonal scale) decreases in the Asturian, Western Paris and Lusitanian basins whereas it increases in northern European basins. Additionally, a gap in the belemnite record is observed in many locations at the beginning of the T-OAE, with regional-dependent duration (e.g., Rocha et al., 2016; Duarte et al., 2017; Ullmann et al., 2020; Rita et al., 2021).

Global changes in ocean element chemistry accompanied the early Toarcian warming and 2nd-order mass extinction (e.g., Jenkyns, 2010; Ruhl et al., 2016; Silva et al., 2021b; Thibault et al., 2018). The concentration and distribution of trace elements in seawater are mainly controlled by external sources, e.g., riverine input, wind-blown dust, volcanism, and hydrothermal circulation at mid-ocean ridges, and internal abiological and biological oceanic and depositional recycling processes (e.g., Emerson and Hedges, 2008; Trujillo and Thurman, 2017). Understanding how the oceanic element inventory responded to the various Late Pliensbachian and Early Toarcian environmental events is crucial in gaining new insights into the relationship between hyperthermals, biological stress and extinction dynamics, and the T-OAE drivers (De Baets et al., 2021; Nätscher et al., 2021; Rita et al., 2019; Ullmann et al., 2020; Ullmann et al., 2014). These insights can help us better understand ecosystem dynamics during this time and other periods of significant environmental upheaval.

Usually, paleo-ocean element chemistry has been mostly inferred from rock inventories (Algeo and Tribovillard, 2009; Bennett and Canfield, 2020; Dickson et al., 2017; Percival et al., 2016; Thibault et al., 2018; Tribovillard et al., 2012; Tribovillard et al., 2006). The limitation of this kind of bulk analysis resides in the difficulty of separating the primary seawater element chemistry from authigenic, biogenic, allogenic (detrital) and diagenetic components (Kovács et al., 2024; Silva et al., 2021b; Thibault et al., 2018). One way of circumventing the limitation of using rock chemistry is to analyze biogenic carbonate, as the element composition of mineralized tissues in several marine species is thought to reflect the composition of seawater and indirectly allow to record, directly or indirectly, changes in element inventories (Armendáriz et al., 2013; Gómez et al., 2008; Gómez and Goy, 2011; Korte and Hesselbo, 2011; I Rosales et al., 2004a; Rosales et al., 2001; Ullmann et al., 2020, Ullmann et al., 2014; Ullmann and Korte, 2015; van de Schootbrugge et al., 2005).

Belemnites were a group of coleoid cephalopods common from the mid-Sinemurian (Early Jurassic) until their extinction in the end-Cretaceous (Hoffmann and Stevens, 2020). Because their rostra are fairly resistant to diagenesis (e.g., (Immenhauser et al., 2016; Ullmann and Korte, 2015) these carbonate fossils have been intensively used for paleo-oceanographic studies of the Jurassic and Cretaceous. To address the question of how seawater chemistry changed in the European Epicontinental Seaway (Fig. 1) during the Early Toarcian warming, 2nd-order mass extinction, and associated perturbations to the global carbon cycle, the objectives of this paper are to (1) obtain a record of 69 elements from 15 Upper Pliensbachian–Lower Toarcian belemnite rostra from the West Rodiles section in the Asturian Basin, North Spain, (2) discuss the usefulness of these data in discriminating primary (paleo-oceanographic) element seawater signatures, and (3) examine if belemnite major, minor, and trace element chemistry can be used to add to the growing body of information on the known drivers of the T-OAE and associated paleo-oceanographic processes. The belemnite record from northern Spain is particularly interesting as it straddles the T-OAE (which is not the case in other locations such as the Lusitanian Basin, Portugal) and shares commonalities with both the Lusitanian and Normandy and UK basins (e.g., De Baets et al., 2021; Rita et al., 2021; Rita et al., 2019).

## 2. Geological setting

The Asturian Basin (Fig. 1) is an intraplate basin part of the North Iberian continental margin, linked to extensional faulting processes preceding the opening of the Bay of Biscay (Lepvrier and Martínez-García, 1990). This basin contains a thick Paleozoic basement, covered by a gently deformed Mesozoic succession deposited during a Late Triassic–Early Jurassic passive margin stage and a Late Jurassic–Early Cretaceous rifting stage (Aurell et al., 2002; Gómez et al., 2019; Valenzuela, 1988). The basin was deformed during the Cenozoic as the westward continuation of the Pyrenees. During Alpine deformation, a mid-crustal detachment transferring orogenic shortening southward toward the Spanish Central System (Fig. 1a) involved the entire Iberian Plate (Quintana et al., 2015).

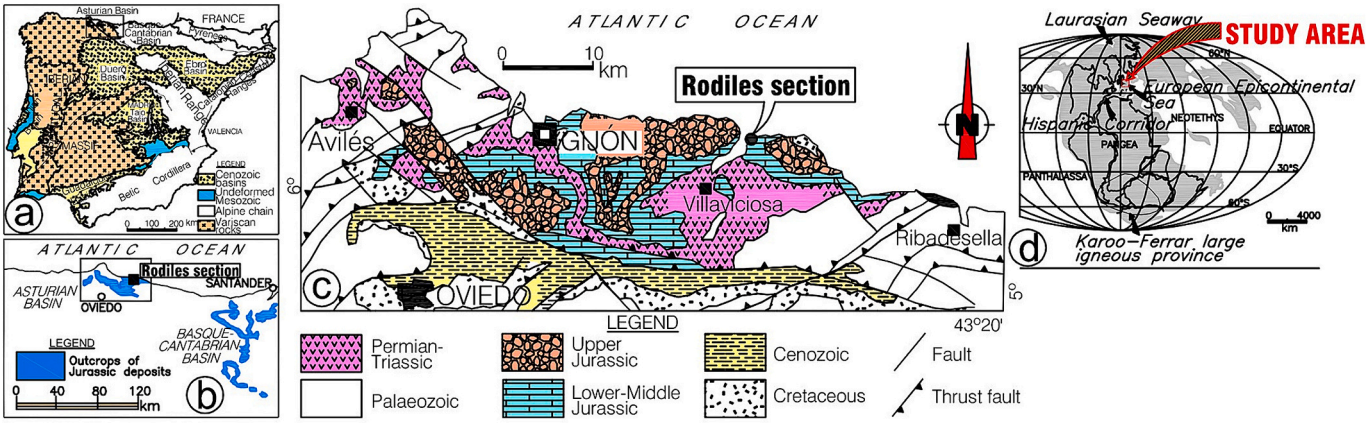


**Fig. 1.** Location of the Asturian Basin and the Rodiles section. a) Sketch map showing the main geological units of Iberia (Spain and Portugal). b) Outcrops of the Lower–Middle Jurassic deposits of Northern Spain. c) Geological map of the Eastern part of the Asturian Basin, showing the location of the Rodiles section. d) Paleogeography of the Lower Jurassic (modified after Golonka, 2007). Iberia was a portion of the European Epicontinental Sea, connected to the North through the Laurasia Seaway and the West through the Hispanic Corridor. In the South, the Karoo-Ferrar LIP represented the main volcanic province during the Pliensbachian and Toarcian stages.

In the Early Jurassic, the Asturian Basin was in a critical position between the Mediterranean Tethys and the Boreal North Atlantic realms (Fig. 1d). In the coastal cliffs of the eastern part of the Asturias region (Fig. 1b and c), well-exposed Upper Pliensbachian–Lower Toarcian deposits consist of alternating lime mudstones and marls belonging to the Santa Mera Member of the Rodiles Formation (Figs. 2 and 3) (Valenzuela, 1988; Valenzuela et al., 1986). Ammonites are abundant, and ammonite-based chronostratigraphic subdivision of the Pliensbachian and Toarcian deposits in Asturias has been updated over the past decades (Aurell et al., 2003; Aurell et al., 2002; Comas-Rengifo et al., 2023; Comas-Rengifo and Goy, 2010; García-Ramos et al., 2010; Gómez et al., 2008; Gómez and Goy, 2011; Suárez Vega, 1974). Standard ammonite chronozones (ACZ) and subchronozones (ASCZ) used in this work correspond with the previously established by Elmi et al. (1997) and Page (2003) for the Northwest Europe and the Submediterranean provinces, respectively.


**Fig. 2.** Field view of the West Rodiles section. The beds closer to the observer correspond to the Upper Pliensbachian Spinatum ACZ, and the cliffs in the background to the Bifrons and lowermost Variabilis ACZ's. The red rocks in the background are from the Kimmeridgian, deposited in fluvial environments. (For interpretation of the references to colour in this figure legend, the reader is referred to the web version of this article.)

### 2.1. The West Rodiles section

The West Rodiles section (Figs. 1–4) offers excellent exposure of the Pliensbachian–Toarcian succession, bearing frequent ammonites that allow precise biostratigraphical subdivisions to be applied (Comas-Rengifo et al., 2023; Gómez et al., 2008; Gómez and Goy, 2011). The section is located about 10 km northeast of Villaviciosa village and comprises about 25 m of the Rodiles Formation. It consists of grey limestones and grey marls dated from the Spinatum and Tenuicostatum (Lower Toarcian) ACZs. A laminated organic-rich dark grey marly interval is observed at the Tenuicostatum/Serpentinum ACZs boundary, surpassing 3 wt% total organic carbon (TOC) (Gómez et al., 2016a; Rodrigues et al., 2020c). The Serpentinum ACZ comprises alternating bioturbated grey marly limestones with grey marls. Macro and microfossils are abundant in most of the section, presenting large changes in the Lower Toarcian. The Early Toarcian extinction was recognized here.

Based on the works of Gómez and Goy (2011) and Fraguas et al. (2012), the Lower Toarcian extinction interval in the study area comprises the uppermost Upper Pliensbachian Spinatum ACZ and the Lower Toarcian Tenuicostatum ACZ and the NJ5 and the lowermost NJ6 Calcareous Nannofossil Zones (CNZ). The extinction boundary is located around the Tenuicostatum/Serpentinum ACZs boundary and within the NJ6 CNZ, and the repopulation interval starts above the extinction boundary and extends beyond the top of the studied part of the section (Fig. 4).

### 2.2. Stable carbon and oxygen isotope geochemistry and chemostratigraphy

Stable carbon and oxygen isotope geochemistry of belemnite and bulk rock carbonate and kerogen have been conducted at the West Rodiles section (Gómez et al., 2016b; Gómez et al., 2008; Gómez and Goy, 2011; Rodrigues et al., 2020c) (Fig. 4). Belemnite rostrum $\delta^{18}O$ values are progressively more negative from the uppermost Pliensbachian, recording the Late Pliensbachian cooling through the lowermost Toarcian Tenuicostatum ACZ. A shift toward more negative values starts at the Tenuicostatum ACZ, reaching a peak value around −2.9 ‰ in the Elegantulum ASCZ. Temperature inferences from belemnite $\delta^{18}O$ suggest significant seawater warming at this time, which includes the extinction boundary and continues through the Serpentinum and the Bifrons ACZ. Overall, seawater temperature is thought to have started to increase in the earliest Toarcian and increased considerably around the Tenuicostatum–Serpentinum zonal boundary.

The $\delta^{13}C$ curve from belemnite carbonate describes a generally

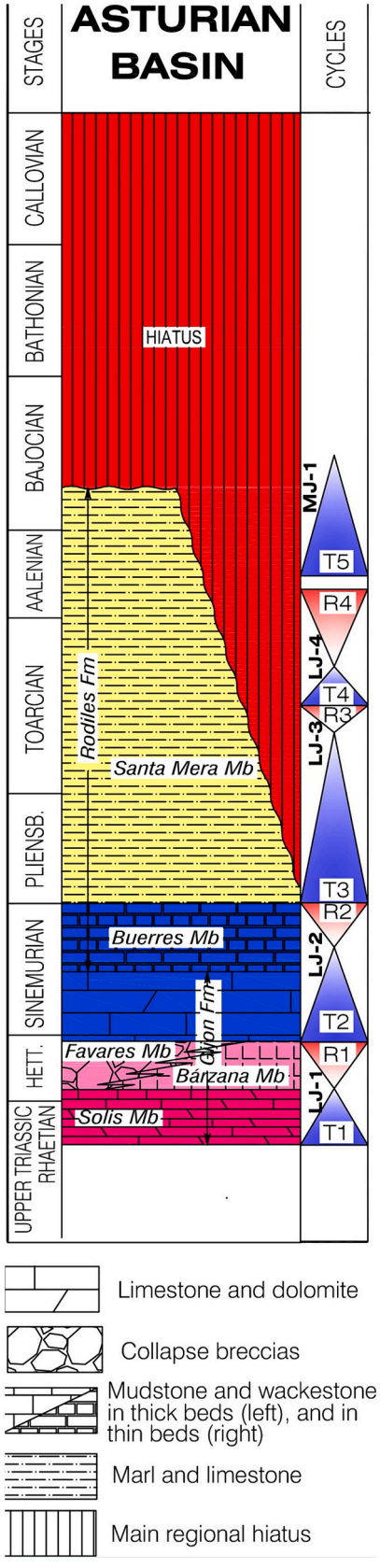


**Fig. 3.** Regional stratigraphy of the Jurassic units of the Asturian Basin. The studied deposits correspond to the Santa Mera Member of the Rodiles Formation (modified after Gómez et al., 2019). The hiatus is a regional feature of the Asturian Basin.

positive trend, with the most frequent values between 0 and + 2‰. A maximum of ~3.25 ‰ is reached in the Elegantulum ASCZ of the Serpentinum ACZ, decreasing upwards to negative values in the Bifrons ASCZ. The positive $\delta^{13}C_{bel}$ trend is interrupted by several minor negative excursions. The oldest is a ~ 2‰ negative shift below the Pliensbachian–Toarcian boundary. A negative peak of similar magnitude is in the Bifrons ASCZ. Other minor negative peaks are located at different parts of the section. However, the T-OAE negative CIE is not recorded in the belemnite dataset, as is also the case in the UK (van de Schootbrugge et al., 2005). The $\delta^{13}C_{carb}$ and $\delta^{13}C_{kerogen}$ curves show a different trend. The most significant feature is a $\delta^{13}C$ negative shift of ~2 ‰ in bulk rock and ~ 8 ‰ in kerogen at the Tenuicostatum–Serpentinum ACZ boundary, coinciding with the extinction boundary and the organic-rich laminated shale facies; this is interpreted to correspond to the T-OAE negative CIE.

A chronostratigraphic equivalency to the T-OAE interval, as recorded in northern Europe (Fig. S1), is shown in Fig. 4. The chronostratigraphic interval equivalent to the T-OAE is about 5 m thick; the base is well defined, whereas the top cannot be confidently pinned. The recognition of the T-OAE interval in West Rodiles is based on TOC and $\delta^{13}C$ (bulk rock and kerogen) chemostratigraphic correlation to Mochras (UK, Fig. S1) and other neighbouring sections (Gómez and Goy, 2011; Rodrigues et al., 2020c; Silva et al., 2021a; Storm et al., 2020) and is supported by ammonite and calcareous nannofossil biostratigraphy. Total organic carbon contents max out at around 3 wt%, indicating that they do not correspond to black shales but are organic-rich facies contemporaneous with Organic Matter Preservation Interval T4 (OAE) (Fig. S1, cf., Silva et al., 2021a).

## 3. Materials and methods

A total of 15 sample aliquots of belemnite rostra from the West Rodiles section of the Asturian Basin in North Spain were selected for ultra-trace element analysis from the studies of Gómez et al. (2008) and Gómez and Goy (2011). Burial diagenesis of the selected belemnite rostrum sample aliquots was tested previously using a combination of cathodoluminescence and stable carbon and oxygen isotopes (Gómez et al., 2008; Gómez and Goy, 2011). In these studies, polished samples and thick sections of each belemnite were prepared and studied under the petrographic and the cathodoluminescence microscope. Only the non-luminescent portions of the belemnite rostra were sampled using a microscope-mounted dental drill to avoid visible diagenetic-altered calcite; this included the apical line and boarders of the sample specimens (Fig. 5). Other chemical proxies of diagenetic alteration from this study are discussed in section 5.1.

A total of 69 elements were selected for analysis, i.e., Ag, Al, As, Au, B, Ba, Be, Bi, Br, Ca, Cd, Ce, Co, Cr, Cs, Cu, Dy, Er, Eu, Fe, Ga, Gd, Ge, Hf, Ho, I, Ir, K, La, Li, Lu, Mg, Mn, Mo, Na, Nb, Nd, Ni, Os, P, Pb, Pd, Pr, Pt, Rb, Re, Ru, S, Sb, Sc, Se, Si, Sm, Sn Sr, Ta, Tb, Te, Th, Ti, Tl, Tm, U, W, V, Y, Yb, Zn, Zr. Element concentration was determined at ALS Scandinavia AB labs. Powdered samples were digested using MW-assisted digestion with concentrated $HNO_3$ (purified by sub-boiled distillation). Digests were analyzed by Inductively Coupled Plasma-Sector Field Mass Spectrometry (ICP-SFMS, Element XR from Thermo Scientific) using a combination of internal standardization and external calibration. The certified reference material JB-2 basalt from the Geological Survey of Japan was used as quality control with acceptance criteria of recoveries within the 90–110% range for elements with accredited concentrations and within the 80–120% range for elements with published concentrations. Level of Reporting (LORs) were calculated as 3 sigma (σ) from preparation blanks. Results are reported in μg/kg (ppb). After analysis of the 69 selected elements, 15 (i.e., Au, Be, Br, Eu, Ga, Ge, Hf, Ir, Nb, Os, Pd, Pt, Re, Ru, Ta) were not further considered since the concentration in 4 or more samples was below the limit of reporting (LOR) (Table S1).

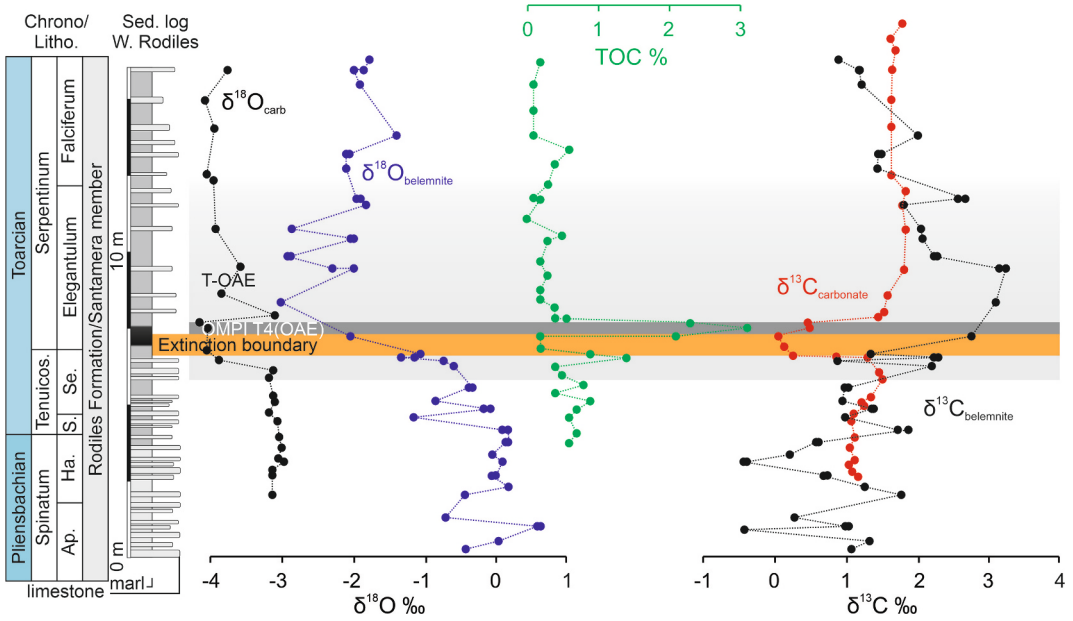


**Fig. 4.** Stratigraphic log of the West Rodiles section (modified after Gómez and Goy, 2011), showing $\delta^{18}O$ and $\delta^{13}C$ values from belemnite calcite and bulk carbonate, as well as total organic carbon (TOC) (Data from (Gómez et al., 2016a).

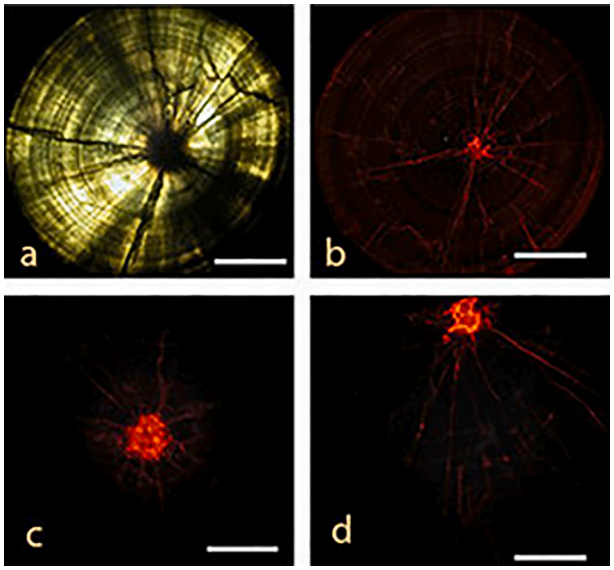


**Fig. 5.** Photomicrographs of some of the belemnite rostra samples under optical (a) and cathodoluminescent microscope (b, c, d). Luminescence in the apical lines and microfractures indicates the presence of diagenetic alteration in these parts. Non-luminescent dark parts indicate the absence of diagenetic alteration, where the samples were drilled for analysis. Rostra (a) and (b) come from Serpentinum ACZ, Murleyi ASCZ. Rostra (c and d) correspond to the Upper Pliensbachian Hawskerense ACZ.

## 4. Results

### 4.1. Elemental composition

Plotting of element concentration and element/Ca against stratigraphic horizons (Figs. 6 and 7 and Fig. S2) reveals four general modes of element distribution in relation to the extinction boundary, the OMPI T4 (OAE), and the chronostratigraphic equivalent of the T-OAE interval:

1) Increasing concentration in the T-OAE with maxima after the extinction boundary and the OMPI T4 (OAE) (Al, As, Ba, Co, Cr, Mg, Mn, P, Sr, Tl).
2) Spiking element concentrations just below and above the extinction boundary and the OMPI T4 (OAE) (Cd, Ce, Cs, Dy, Er, Gd, Ho, La, Lu, Nd, Pr, S, Sc, Sm, Tb, Th, Tm, U, V, Y, Yb).
3) Decreasing element concentrations from the base to the top of the studied interval (B, Bi, Fe, I, K, Li, Na, Rb, Ti, Zr).
4) Minima element concentrations below and above the extinction boundary and the OMPI T4 (OAE) or no major change (Ag, Ca, Cu, Mo, Ni, Pb, Sb, Se, Si, Sn, Te, W, Zn).

## 5. Discussion

### 5.1. Screening of diagenetic alteration and preservation of element geochemistry in belemnites

Previous $\delta^{18}O$ studies (Gómez et al., 2008; Gómez and Goy, 2011) on the same belemnite rostra show "normal" marine values, suggesting the absence of strong diagenetic alteration of belemnite calcite. In the $\delta^{18}O_{bel}$ vs $\delta^{13}C_{bel}$ plot, data group into a cluster-type distribution, supporting the inference that belemnite calcite largely resisted diagenesis. Looking at elements typically used for geochemical diagenetic screening of belemnites, i.e., Fe, Mn, and Sr and their ratios to Ca, samples WR-42 and WR-47 were excluded from further consideration since they seem to be diagenetically altered (Table 1).

Another issue that could affect belemnite calcite chemistry relating to diagenesis is the influence of changes in lithology in belemnite rostrum preservation. The influence of changes in lithology/preservation seems limited, at least on studies focusing on the size and diversity of belemnites from different nearby sections (Rita et al., 2018). However, changing lithology can potentially influence element concentrations, either directly affecting rostrum calcite or by inducing the precipitation of different impurities and cements (contamination in a broad sense). The impact of contamination is discussed below per section.

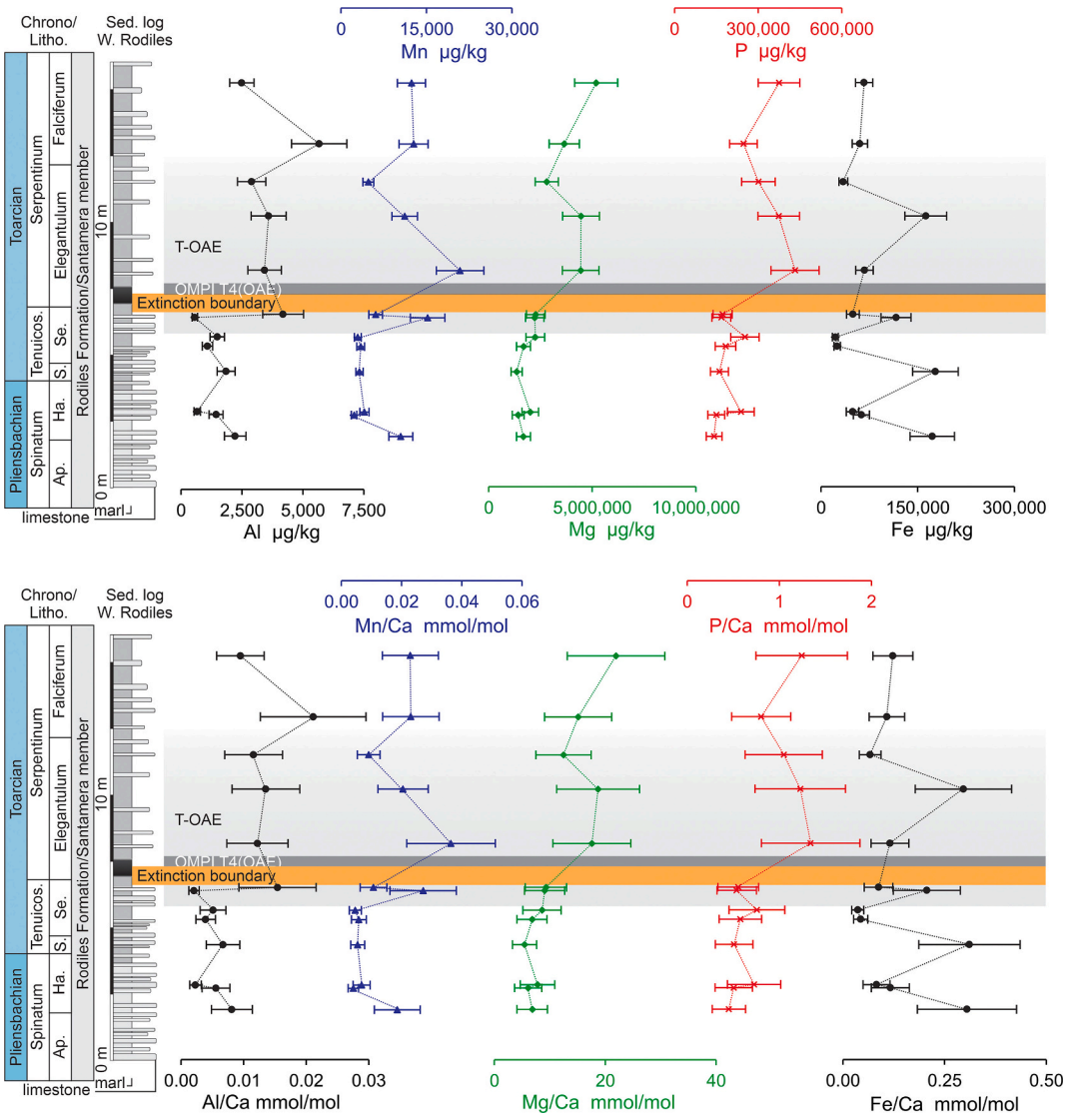


**Fig. 6.** Stratigraphic log of the West Rodiles section (modified after Gómez and Goy, 2011) and stratigraphic distribution of major elements and element/Ca determined in belemnite calcite.

### *5.2. Late Pliensbachian–Early Toarcian ocean chemistry recorded in belemnite rostra*

For belemnite rostra element geochemistry to be a reliable indicator for past seawater composition, the abundance of a given element needs to depend mainly on seawater composition, and the processes that govern element incorporation into biogenic carbonate need to be well understood and validated using modern analogues. Therefore, because belemnites lack a modern analogue, reconstruction of the "absolute" chemistry of Late Pliensbachian–Early Toarcian oceans from belemnites is severely hindered. Usually, belemnite rostra geochemical studies rely on calibrations with specimens of other taxa with modern analogues, adding uncertainty in interpretations (Immenhauser et al., 2016; Ullmann et al., 2015; Ullmann et al., 2013; Ullmann and Korte, 2015).

Living systems are built from a small subset of the atomic elements, including macronutrients (C, H, N, O, P, S) and ions (Mg, K, Na, Ca) together with a small but variable set of trace elements (micronutrients) (Remick and Helmann, 2023). Element incorporation into biogenic carbonates, including belemnites, can be affected by the influence of several environmental and physiological factors (Hoffmann and Stevens, 2020; Ullmann and Korte, 2015), in addition to intra-species differences (e.g., McArthur et al., 2007; Li et al., 2013). Regarding the latter, previous studies noted intra-rostral variations and inter-species/genus differences in the incorporation of several elements, e.g., Mg and Na (McArthur et al., 2007; Wierzbowski and Joachimski, 2007; Li et al., 2012). On the other hand, Sr seems to be less sensitive to this effect (Ullmann and Pogge von Strandmann, 2017). Although debate remains regarding the original mineralogy and organic matter content, it is generally thought that belemnite rostra is comparable to the Sepia cuttlebone sheath (Hoffmann and Stevens, 2020). However, in vivo studies of Sepia are rare and have contradictory inferences regarding the influence of temperature (i.e., Sr, Mn), growth rates (i.e., Li), and diet (i.e., Sr, Ba, Mn, Y) in element incorporation into Sepia bio-carbonate, i.e., statoliths and cuttlebone (Chung et al., 2020a, 2020b; Zumholz et al., 2006). Other studies have reported population or geographic differences in cuttlebone element chemistry (Ikeda et al., 1999; Turan and Yaglioglu, 2010).

Below, we assess if belemnite rostra element chemistry reflects broad and relative changes in paleo seawater chemistry (e.g., Ullmann et al., 2013). The impact of (1) vital effects (i.e. growth rate, ontogeny, and species-specific fractionation, (2) Early Toarcian faunal turnover and (3) consideration of analytical uncertainty is also discussed below in each section.

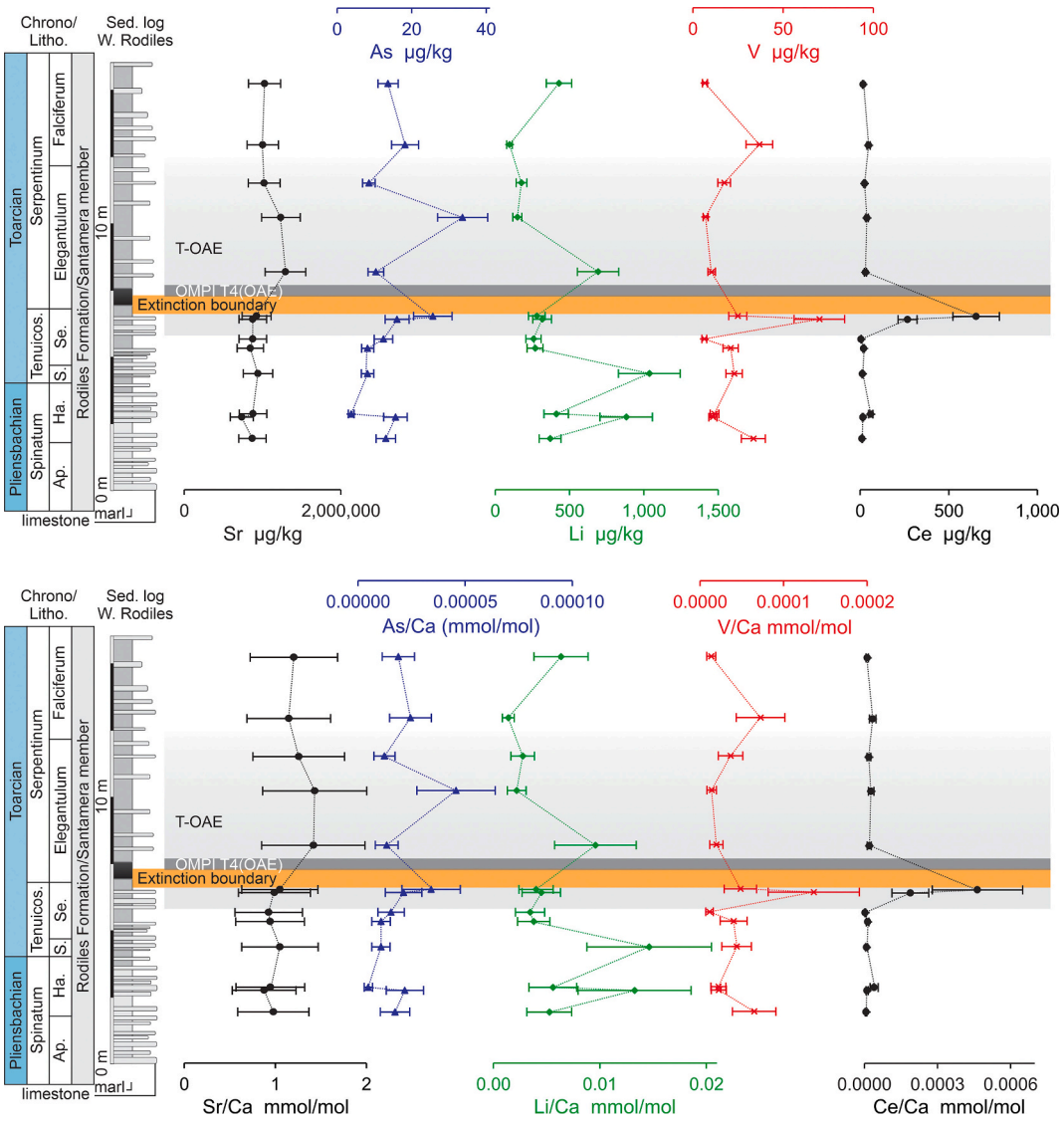


**Fig. 7.** Stratigraphic log of the West Rodiles section (modified after Gómez and Goy, 2011) and stratigraphic distribution of minor and trace elements and element/Ca determined in belemnite calcite.

### 5.2.1. *Unresolved elements*

Several elements (1: Al, As, Ba, Co, Cr, Tl; Mode 2: Cd, Ce, Cs, Dy, Er, Gd, Ho, La, Lu, Nd, Pr, Sc, Sm, Tb, Th, Tm, U, V, Y, Yb; 3: B, Bi, I, Li, Rb, Ti, Zr; 4: Ag, Cu, Mo, Ni, Pb, Sb, Se, Si, Sn, Te, W, Zn) are determined in the extremely low ppm-ppb range (below ~30 ppm, often in the low ppb range). These low contents do not allow us to confidently discard that the observed trends do not include contamination or alteration of original values that cannot be resolved using stable carbon and oxygen isotopes or standard element chemistry screening techniques. Contamination could, in this case, refer to microscopic amounts of other minerals/organic matter incorporated into belemnite rostra in microfractures. The above, combined with the lack of literature regarding the incorporation of these elements into belemnite calcite, do not allow us to confidently assign the observed trends of these elements to changes in ocean chemistry. Therefore, we report these elements, but they will not be further considered. For elements in the list above that are present in larger amounts, the lack of variation precludes assignment to seawater chemistry directly; either the element's seawater chemistry did not change markedly, or the incorporation of these elements could have been biologically buffered, due to inter-species effects, or diagenetically affected in a way that is not detected using commonly used screening techniques.

### 5.2.2. *Early Toarcian acceleration of the hydrological cycle*

Magnesium, Mn, P, and Sr increase concentration in the T-OAE chronocorrelative interval with maxima after the extinction boundary and the OMPI T4 (OAE) (Figs. 6, 7 and Figs. S1 and S2).

Some of these elements, such as Mg, Mn, and P, are biologically essential. The inclusion of Mg and Sr in this group facilitates their assignment and interpretation as the incorporation of these two elements into belemnite carbonate has been amply discussed (McArthur et al., 2000; Rosales et al., 2001, 2004a; Rosales et al., 2004b; van de Schootbrugge et al., 2005; McArthur et al., 2007; Korte and Hesselbo, 2011; Li et al., 2012, 2013; Ullmann et al., 2013, 2014, 2015; Ullmann and Korte, 2015; McArthur et al., 2020).

Although Mg and Sr have been used as paleothermometers in belemnite (e.g., Li et al., 2012; Rosales et al., 2004a), Mg incorporation was shown to have an intra-species dependency component, whereas Sr seems much less affected (e.g., Li et al., 2013; McArthur et al., 2007). Other vital effects, such as growth rate, seem to be of minor importance for the broad, large-scale variability of Mg/Ca and Sr/Ca in belemnite rostra (Ullmann and Pogge von Strandmann, 2017). It was suggested that Sr/Ca of fossil low-Mg calcite mainly reflects ocean water chemistry since intra-specific effects in Sr are minor (McArthur et al., 2007), and a relationship with temperature or growth rate is not clear (Ullmann and

**Table 1**
Calcium, Fe, Mn, and Sr contents and their rations with Ca from the West Rodiles Section of the Asturian Basin (Northern Spain) and used cutoff limits for the discrimination of diagenetically altered samples.

| Sample | Ca mg/kg | Fe mg/kg | Mn mg/kg | Sr mg/kg | Fe/Ca mmol/mol | Mn/Ca mmol/mol |
|---|---|---|---|---|---|---|
| WR-14 | 406,088 | 172 | 10 | 870 | 0.3 | 0.02 |
| WR-17 | 383,878 | 62 | 2 | 736 | 0.12 | 0.00 |
| WR-21 | 424,242 | 49 | 4 | 877 | 0.08 | 0.01 |
| WR-31 | 409,565 | 177 | 3 | 941 | 0.31 | 0.01 |
| WR-37 | 409,180 | 25 | 3 | 844 | 0.04 | 0.01 |
| WR-39 | 431,940 | 22 | 3 | 876 | 0.04 | 0.00 |
| WR-42 | 411,678 | 930 | 50 | 882 | 1.62 | 0.09 |
| WR-43.1 | 404,903 | 116 | 15 | 876 | 0.21 | 0.03 |
| WR-43.2 | 403,137 | 49 | 6 | 925 | 0.09 | 0.01 |
| WR-45t | 416,934 | 67 | 21 | 1293 | 0.12 | 0.04 |
| WR-47 | 376,637 | 443 | 50 | 950 | 0.84 | 0.10 |
| WR-49 | 393,689 | 163 | 11 | 1234 | 0.3 | 0.02 |
| WR-53 | 371,039 | 35 | 5 | 1021 | 0.07 | 0.01 |
| WR-58 | 398,874 | 60 | 13 | 1002 | 0.11 | 0.02 |
| WR-65 | 389,738 | 67 | 12 | 1026 | 0.12 | 0.02 |
| limits | | <250[#] | <32[#] | >400[&] | <0.45[+] | <0.10* |

References: [#] Rosales et al., 2001; [&] Korte and Hesselbo, 2011; [+] Rosales et al., 2004a; * Ullmann et al., 2014, 2020

Pogge von Strandmann, 2017; Ullmann et al., 2013; Ullmann and Korte, 2015). Ullmann and Pogge von Strandmann (2017) observed that average Sr/Ca and Mg/Ca show large changes for Toarcian whole belemnite specimens, especially across the T-OAE, and these changes are larger than the intra-specimen and intra-generic variability from several studies. This suggests that broad changes in these ratios can represent forcing from external signals, i.e., changing temperatures or sea-water chemistry (e.g., Li et al., 2012; I Rosales et al., 2004b, Rosales et al., 2004a).

Ullmann et al. (2013) argued that the Early Toarcian increase in Sr/Ca and $^{87}Sr/^{86}Sr$ can be explained by enhanced silicate weathering on the continents induced by the Karoo and Ferrar LIP volcanism (e.g., Cohen and Coe, 2007; Hesselbo et al., 2007; Percival et al., 2016; Percival et al., 2015; Ruhl et al., 2022; Storm et al., 2020). In the Asturian Basin, the TOAE negative CIE interval (Figs. 4, 6, and 7) includes the extinction boundary of Gómez et al. (2016b) and Gómez and Goy (2011) It is marked by a negative CIE (recorded in $\delta^{13}C$ of kerogen and bulk rock) associated with the highest TOC, total sulphur, and amorphous organic matter contents (Gómez and Goy, 2011; Rodrigues et al., 2020c). It was interpreted that deposition and preservation of organic matter during the TOAE interval in the study area occurred under, at least, suboxic conditions and that the occurrence of non-opaque phytoclasts and terrestrial palynomorphs could represent an increase in continental weathering and fluvial runoff in warmer/wetter conditions resulting from the Early Toarcian acceleration of the hydrological cycle (Rodrigues et al., 2021; Rodrigues et al., 2020c). In the Asturias Basin and other winter-wet/warm temperate climatic belt basins, the observed enrichment of AOM probably reflects an increase in primary productivity linked to increased continental weathering, fluvial runoff and riverine organic matter owing to nutrient input into marine areas (Rodrigues et al., 2021, Rodrigues et al., 2020c).

Even though sampled belemnite specimens were not identified to the species level, ontogenetic stage was not considered fully (however, apical areas were avoided during sampling due to the high likelihood of diagenetic alteration), and the dataset spans a known event of belemnite fauna turnover, published literature supports the inference that the broad, long term trends of Sr (and Mg even considering intra-species fractionation) likely reflect broad changes in seawater chemistry. Based on the general oceanographic proprieties of several elements that show the same trends as Sr, it is possible that the observed Mn and P trends result from the same set of processes, that is, increased continental weathering and fluvial runoff of these elements into the area due to acceleration of the hydrological cycle associated with the Early Toarcian carbon cycle perturbation and warming (see also -Ullmann et al., 2013). Further studies must address whether intra-specimen variation and ontogenetic stage impact the incorporation of Mn and P into belemnites.

#### 5.2.3. Decoupling of the Fe and Mn Ocean cycles

Several elements showing decreasing element concentrations from the base to the top of the studied interval (Fe, K, and Na, Fig. 7 and Fig. S2) are often associated with external inputs into the ocean, such as dust, riverine sediments, sediment dissolution along continental margins, and fluids from hydrothermal vents (Poehle and Koschinsky, 2017; Zheng et al., 2022). Regardless of their source (discrimination is beyond the scope of this paper), since K and Fe are essential for many organisms, their decreasing trend upward in the section may suggest that low seawater K and Fe contents might have been a limiting factor of oceanic productivity in the area, probably explaining why organic-rich facies in the Asturian Basin are limited to the base of the T-OAE, i.e., OMPI T4 (OAE) of Silva et al. (2021b).

Speculatively, low seawater Fe content at the top of the study intervals could arise either from (1) high reactivity in the presence of oxygen (higher than Mn) and increased preservation of authigenic clays, pyrite, and Fe oxides in sediments or (2) decreased external inputs, i.e., riverine, and wind-blown dust (Jensen et al., 2020). Considering the overall lithological Fe-rich context of several locations around Iberia during and after (?) the T-OAE [e.g., the Chocolate Marls of the Lusitanian Basin (Duarte, 2007; Pittet et al., 2014; Rodrigues et al., 2016), the Zegrí Formation of the Betic Cordillera (Silva et al., 2021b), and the siderite-rich Mochras borehole in Cardigan Bay Basin (Xu et al., 2018)] and evidence of an accelerated hydrological cycle in the area (e.g., (Rodrigues et al., 2021, Rodrigues et al., 2020a, 2020b, 2020c, Rodrigues et al., 2019)], the former mechanism is preferred in this study. Decoupling of the Fe and Mn cycling in the oceans is a common feature of the geological record. Recognizing that these two crucial ocean biogeochemical cycles can decouple has important implications for understanding how other metals are scavenged throughout the water column (Jensen et al., 2020).

### 5.3. Relationship between inferred elemental ocean chemistry and biocalcification in belemnites and calcareous nannofossils

As aforementioned, the Early Toarcian was a time interval of important biological perturbation in the global ocean. Several calcareous nannofossils species, e.g. *Schizosphaerella punctulata*, *Biscutum* spp., *Similiscutum* spp. or *Lotharingius* spp., experienced size reduction and morphological changes during this time interval (e.g., (Clémence et al., 2014; Faucher et al., 2022; Ferreira et al., 2017; Fraguas et al., 2012; Fraguas and Young, 2011; Mattioli et al., 2004; Peti and Thibault, 2017; Suan et al., 2008). A biometric analysis of the genus *Lotharingius* in the studied section by (Fraguas and Young, 2011) found a decrease in size or "dwarfing" of the analyzed *Lotharingius* species in samples corresponding to the T-OAE negative CIE. They hypothesize that the reduction in size and abundance was related to unfavourable paleoenvironmental conditions for the biomineralization of their coccoliths. The reduction in size of nannofossils contrasts with belemnites. In the studies section, a general increase in belemnite median rostrum size is seen due to the appearance of new and larger taxa associated with a marked taxonomic turnover, whereas total belemnite diversity decreases (De Baets et al., 2021; Rita et al., 2021). The causes for these discrepancies between groups need to be considered in future studies.

Considering the results obtained from belemnite rostra geochemistry from our study, there is a correspondence between an increase in Mg, Mn, P, and Sr and a decrease in Fe, K, and Na around the extinction

boundary (cf. Fraguas et al., 2012; Gómez and Goy, 2011) and the T-OAE negative CIE and the previously observed reduction size or dwarfism of *Lotharingius* in Rodiles. This observation adds new insights to the ongoing discussion on the factors (such as $pCO_2$, ocean acidification, and seawater warming) contributing to the so-called Early Jurassic calcareous nannofossil crisis (Clémence et al., 2015; Clémence et al., 2014; Ferreira et al., 2017; Mattioli et al., 2009b) or patterns of belemnite evolution in the Early Jurassic (De Baets et al., 2021; Neige et al., 2021). Parallel to our empirical observation between nannofossil dwarfing and changing ocean chemistry with respect to Mg, Mn, P, Sr, Fe, K, and Na, a recent study by Faucher et al. (2017) found a negative effect of several trace elements on nannoplankton biocalcification processes. They demonstrate this effect using four living coccolithophore species, *Emiliania huxleyi, Gephyrocapsa oceanica, Pleurochrysis carterae* and *Coccolithus pelagicus*, by control culture and metal-enriched (V, Ni, Zn and Pb) experiments. It was found that coccolith specimens under stress metal-rich conditions display an irregular shape and are thinner, suggesting difficulties in calcification under metal-enriched conditions.

## 6. Conclusions

This study presents and discusses a dataset comprising the geochemical determination of 69 elements in 13 diagenetic screened belemnite rostra from the Upper Pliensbachian–Lower Toarcian West Rodiles section, Asturian Basin, Northern Spain.

Discarding large intra-species effects and assuming a similar influence of growth rates, diet, and other physiological processes for all analyzed belemnite rostra and taking into consideration analytical uncertainty, we assessed if belemnite rostra element chemistry reflects broad and relative changes in paleo seawater chemistry during the Late Pliensbachian and Early Toarcian and concluded:

1) Elements such as Mg, Mn, P, and Sr increase across the T-OAE chronocorrelative interval and have elevated contents after the extinction boundary and the OMPI T4 (OAE). Supported by previous studies on Sr and Mg incorporation into belemnite carbonate, this trend is interpreted to likely represent an increase of these elements' inventory in regional seawater due to an increase in continental weathering and fluvial runoff into the area due to acceleration of the hydrological cycle associated with the Early Toarcian carbon cycle perturbation and warming.
2) Iron and K decrease upwards in the section. The low paleo-seawater K and Fe contents are interpreted to have been a limiting factor of oceanic productivity in the area, likely explaining why organic-rich facies in the Asturian Basin are limited to the base of the T-OAE. In addition, Fe and Mn show different trends, indicating the decoupling of the Fe and Mn ocean cycles in the study area during the Early Toarcian.
3) Several elements are determined in the low ppm range (below ~30 ppm, often in the low ppb range), and we cannot confidently discard very minor contamination or alteration of original values that are unresolvable using stable carbon and oxygen isotopes or element chemistry screening techniques. Combined with the lack of literature regarding the incorporation of these elements into belemnite rostra calcite, we cannot confidently assign the observed trends of these elements to ocean chemistry. These are reported for future reference.
4) Considering the element geochemistry results from belemnite rostra from our study, there is a correspondence between changing seawater element chemistry around the extinction boundary, warming, the T-OAE negative CIE, marked belemnite turnover and size increase (observed at various sites, including Rodiles), and a reduction in size or dwarfism of *Lotharingius* in the study area. Causes need to be considered in future studies.

Supplementary data to this article can be found online at https://doi.org/10.1016/j.chemgeo.2024.122327.

## CRediT authorship contribution statement

**Ricardo L. Silva:** Writing – review & editing, Writing – original draft, Visualization, Validation, Methodology, Investigation, Funding acquisition, Formal analysis, Data curation, Conceptualization. **Juan J. Gómez:** Writing – review & editing, Writing – original draft, Visualization, Methodology, Formal analysis, Data curation, Conceptualization. **Ángela Fraguas:** Writing – review & editing, Writing – original draft, Investigation.

## Declaration of competing interest

The authors declare that they have no known competing financial interests or personal relationships that could have appeared to influence the work reported in this paper.

## Data availability

Data is given as suplementary data file

## Acknowledgements

Natural Sciences and Engineering Research Council of Canada supports Ricardo L. Silva via a Discovery Grant (grant number RGPIN-2024-04888). A. Fraguas was supported by the research group UCM-900431. We want to express our gratitude to the Editor-in-Chief, Vasileios Mavromatis, and the three reviewers for their valuable feedback, which significantly enhanced this manuscript. This study is a contribution to the UNESCO-IUGS projects IGCP 655 Toarcian Oceanic Anoxic Event: Impact on marine carbon cycle and ecosystems and IGCP 739 The Mesozoic-Palaeogene hyperthermal events.

## References

Algeo, T.J., Tribovillard, N., 2009. Environmental analysis of paleoceanographic systems based on molybdenum–uranium covariation. Chem. Geol. 268, 211–225. https://doi.org/10.1016/j.chemgeo.2009.09.001.

Arias, C., 2006. Northern and Southern Hemispheres ostracod palaeobiogeography during the early Jurassic: possible migration routes. Palaeogeogr Palaeoclimatol Palaeoecol 233, 63–95. https://doi.org/10.1016/j.jaap.2005.12.013.

Arias, C., 2009. Extinction pattern of marine Ostracoda across the Pliensbachian-Toarcian boundary in the Cordillera Ibérica, NE Spain: Causes and consequences. Geobios 42, 1–15. https://doi.org/10.1016/j.geobios.2008.09.004.

Armendáriz, M., Rosales, I., Bádenas, B., Piñuela, L., Aurell, M., García-Ramos, J.C., 2013. An approach to estimate lower Jurassic seawater oxygen-isotope composition using δ18O and Mg/ca ratios of belemnite calcites (early Pliensbachian, northern Spain). Terra Nova 25, 439–445. https://doi.org/10.1111/ter.12054.

Aurell, M., Meléndez, G., Olóriz, F., Badenás, B., Caracuel, J.E., García-Ramos, J.C., Goy, A., Linares, A., Quesada, Santiago, Robles, S., Rodríguez-Tovar, F.J., Rosales, I., Sandoval, J., de Centi, C.S., Taverá, J.M., Valenzuela, M., 2002. In: Jurassic, in: Gibbons, W., Moreno, T. (Ed.), The Geology of Spain. Geological Society of London, Unknown, pp. 213–253. https://doi.org/10.1144/GOSPP.11.

Aurell, M., Robles, S., Bádenas, B., Rosales, I., Quesada, S., Meléndez, G., García-Ramos, J.C., 2003. Transgressive-regressive cycles and Jurassic palaeogeography of Northeast Iberia. Sediment. Geol. 162, 239–271. https://doi.org/10.1016/S0037-0738(03)00154-4.

Baeza-Carratalá, J.F., García Joral, F., Giannetti, A., Tent-Manclús, J.E., 2015. Evolution of the last koninckinids (Athyridida, Koninckinidae), a precursor signal of the early Toarcian mass extinction event in the Western Tethys. Palaeogeogr Palaeoclimatol Palaeoecol 429, 41–56. https://doi.org/10.1016/j.palaeo.2015.04.004.

Baeza-Carratalá, J.F., Reolid, M., García Joral, F., 2017. New deep-water brachiopod resilient assemblage from the South-Iberian Palaeomargin (Western Tethys) and its significance for the brachiopod adaptive strategies around the early Toarcian Mass Extinction Event. Bull. Geosci. 92, 233–256. https://doi.org/10.3140/bull.geosci.1631.

Baker, S.J., Hesselbo, S.P., Lenton, T.M., Duarte, L.V., Belcher, C.M., 2017. Charcoal evidence that rising atmospheric oxygen terminated early Jurassic Ocean anoxia. Nat. Commun. 8, 7. https://doi.org/10.1038/ncomms15018.

Bennett, W.W., Canfield, D.E., 2020. Redox-sensitive trace metals as paleoredox proxies: a review and analysis of data from modern sediments. Earth Sci Rev 204, 103175. https://doi.org/10.1016/j.earscirev.2020.103175.

Brazier, J.M., Suan, G., Tacail, T.T., Simon, L., Martin, J.E., Mattioli, E., Balter, V., 2015. Calcium isotope evidence for dramatic increase of continental weathering during the Toarcian oceanic anoxic event (early Jurassic). Earth Planet. Sci. Lett. 411, 164–176. https://doi.org/10.1016/j.epsl.2014.11.028.

Caswell, B.A., Coe, A.L., 2013. Primary productivity controls on opportunistic bivalves during early jurassic oceanic deoxygenation. Geology 41, 1163–1166. https://doi.org/10.1130/G34819.1.

Caswell, B.A., Frid, C.L.J., 2017. Marine ecosystem resilience during extreme deoxygenation: the early Jurassic oceanic anoxic event. Oecologia 183, 275–290. https://doi.org/10.1007/s00442-016-3747-6.

Caswell, B.A., Coe, A.L., Cohen, A.S., 2009. New range data for marine invertebrate species across the early Toarcian (early Jurassic) mass extinction. 1. J. Geol. Soc. Lond. 166, 859–872. https://doi.org/10.1144/0016-76492008-0831.

Chung, M.-T., Chen, C.-Y., Shiao, J.-C., Lin, S., Wang, C.-H., 2020a. Temperature-dependent fractionation of stable oxygen isotopes differs between cuttlefish statoliths and cuttlebones. Ecol. Indic. 115, 106457 https://doi.org/10.1016/j.ecolind.2020.106457.

Chung, M.-T., Huang, K.-F., You, C.-F., Chiao, C.-C., Wang, C.-H., 2020b. Elemental Ratios in Cuttlebone Indicate Growth rates in the Cuttlefish Sepia pharaonis. Front. Mar. Sci. 6 https://doi.org/10.3389/fmars.2019.00796.

Clémence, M.E., Gardin, S., Bartolini, A., 2014. Pattern and timing of the early Jurassic calcareous nannofossil crisis. Palaeogeogr Palaeoclimatol Palaeoecol 411, 56–64. https://doi.org/10.1016/j.palaeo.2014.06.022.

Clémence, M.-E., Gardin, S., Bartolini, A., 2015. New insights in the pattern and timing of the early Jurassic calcareous nannofossil crisis. Palaeogeogr Palaeoclimatol Palaeoecol 427, 100–108. https://doi.org/10.1016/j.palaeo.2015.03.024.

Cohen, A.S., Coe, A.L., 2007. The impact of the Central Atlantic Magmatic Province on climate and on the Sr- and Os-isotope evolution of seawater. Palaeogeogr Palaeoclimatol Palaeoecol 244, 374–390. https://doi.org/10.1016/j.palaeo.2006.06.036.

Comas-Rengifo, M.J., Goy, A., 2010. Caracterización biocronoestratigráfica del Sinemuriense Superior y el Pliensbachiense entre los afloramientos de la Playa Vega y Lastres (Asturias). In: García-Ramos, J.C. (Ed.), Las Sucesiones Margo-Calcáreas Marinas Del Jurásico Inferior y Las Series Fluviales Del Jurásico Superior. Acantilados de La Playa de Vega (Ribadesella). Guía de Campo (Excursión A), V Congreso Del Jurásico de España. Servitec, Oviedo, Spain, pp. 10–18.

Comas-Rengifo, M.J., García-Ramos, J.C., Goy, A., Piñuela, L., Gómez, J.J., Paredes, R., Suárez Vega, L.C., 2023. Stratigraphy and Biochronostratigraphy of the lower Pliensbachian (Jurassic) from the Asturian basin (Northern Spain). Journal of Iberian Geology 49, 73–96. https://doi.org/10.1007/s41513-023-00209-7.

Danise, S., Twitchett, R.J., Little, C.T.S., 2015. Environmental controls on Jurassic marine ecosystems during global warming. Geology 43, 263–266. https://doi.org/10.1130/G36390.1.

De Baets, K., Nätscher, P.S., Rita, P., Fara, E., Neige, P., Bardin, J., Dera, G., Duarte, L.V., Hughes, Z., Laschinger, P., García-Ramos, J.C., Piñuela, L., Übelacker, C., Weis, R., 2021. The impact of the Pliensbachian–Toarcian crisis on belemnite assemblages and size distribution. Swiss J Palaeontol 140, 25. https://doi.org/10.1186/s13358-021-00242-y.

Dera, G., Pellenard, P., Neige, P., Deconinck, J.F., Pucéat, E., Dommergues, J.L., 2009. Distribution of clay minerals in early Jurassic Peritethyan seas: Palaeoclimatic significance inferred from multiproxy comparisons. Palaeogeogr Palaeoclimatol Palaeoecol 271, 39–51. https://doi.org/10.1016/j.palaeo.2008.09.010.

Dera, G., Toumoulin, A., De Baets, K., 2016. Diversity and morphological evolution of Jurassic belemnites from South Germany. Palaeogeogr Palaeoclimatol Palaeoecol 457, 80–97. https://doi.org/10.1016/j.palaeo.2016.05.029.

Dickson, A.J., Gill, B.C., Ruhl, M., Jenkyns, H.C., Porcelli, D., Idiz, E., Lyons, T.W., van den Boorn, S.H.J.M., 2017. Molybdenum-isotope chemostratigraphy and paleoceanography of the Toarcian Oceanic Anoxic Event (early Jurassic). Paleoceanography 32, 813–829. https://doi.org/10.1002/2016PA003048.

Duarte, L.V., 2007. Lithostratigraphy, sequence stratigraphy and depositional setting of the Pliensbachian and Toarcian series in the Lusitanian Basin (Portugal). Ciencias da Terra 16, 17–23.

Duarte, L.V., Silva, R.L., Félix, F., Comas-Rengifo, M.J., Da Rocha, R.B., Mattioli, E., Paredes, R., Filho, J.G.M., Cabral, M.C., 2017. The jurassic of the Peniche peninsula (Portugal): Scientific, educational and science popularization relevance. Revista de la Sociedad Geologica de Espana 30.

Elmi, S., Rulleau, L., Gabilly, J., Mouterde, R., 1997. Toarcien. In: Cariou, E., Hantzpergue, P. (Eds.), Biostratigraphie Du Jurassique Ouest-Européen et Méditerranéen: Zonations Parallèles et Distribution Des Invertébrés et Microfossiles. Group Francais d'Etude du Jurassic, Poitiers, pp. 25–35.

Emerson, S., Hedges, J., 2008. Chemical Oceanography and the Marine Carbon Cycle. Cambridge University Press.

Erba, E., Bottini, C., Faucher, G., Gambacorta, G., Visentin, S., 2019. The response of calcareous nannoplankton to Oceanic Anoxic events: the Italian pelagic record. Bollettino della Società Paleontologica Italiana 1, 51–71.

Faucher, G., Hoffmann, L., Bach, L.T., Bottini, C., Erba, E., Riebesell, U., 2017. Impact of trace metal concentrations on coccolithophore growth and morphology: laboratory simulations of cretaceous stress. Biogeosciences 14, 3603–3613. https://doi.org/10.5194/bg-14-3603-2017.

Faucher, G., Visentin, S., Gambacorta, G., Erba, E., 2022. Schizosphaerella size and abundance variations across the Toarcian Oceanic Anoxic Event in the Sogno Core (Lombardy Basin, Southern Alps). Palaeogeogr. Palaeoclimatol. Palaeoecol. 595, 110969 https://doi.org/10.1016/j.palaeo.2022.110969.

Ferreira, J., Mattioli, E., van de Schootbrugge, B., 2017. Palaeoenvironmental vs. evolutionary control on size variation of coccoliths across the Lower-Middle Jurassic. Palaeogeogr Palaeoclimatol Palaeoecol 465, 177–192. https://doi.org/10.1016/j.palaeo.2016.10.029.

Fraguas, Á., Young, J.R., 2011. Evolution of the coccolith genus Lotharingius during the late Pliensbachian-early Toarcian interval in Asturias (N Spain). Consequences of the early Toarcian environmental perturbations. Geobios 44, 361–375. https://doi.org/10.1016/j.geobios.2010.10.005.

Fraguas, Á., Comas-Rengifo, M.J., Gómez, J.J., Goy, A., 2012. The calcareous nannofossil crisis in Northern Spain (Asturias province) linked to the early Toarcian warming-driven mass extinction. Mar. Micropaleontol. 94–95, 58–71. https://doi.org/10.1016/j.marmicro.2012.06.004.

Fraguas, Á., Gómez, J.J., Goy, A., Comas-Rengifo, M.J., 2021. The response of calcareous nannoplankton to the latest Pliensbachian–early Toarcian environmental changes in the Camino Section (Basque Cantabrian Basin, northern Spain). Geol. Soc. Lond. Spec. Publ. 514, 31–58. https://doi.org/10.1144/SP514-2020-256.

García-Ramos, J.C., Piñuela, L., Vega, L.C.S., 2010. La ritmita de calizas y margas del Pliensbachiense. In: García-Ramos, J.C. (Ed.), Las Sucesiones Margo-Calcáreas Marinas Del Jurásico Inferior y Las Series Fluviales Del Jurásico Superior. Acantilados de La Playa de Vega (Ribadesella). (Guía de La Excursión A) V Congreso Del Jurasico de Espana, pp. 21–40.

Golonka, J., 2007. Late Triassic and early Jurassic palaeogeography of the world. Palaeogeogr Palaeoclimatol Palaeoecol 244, 297–307. https://doi.org/10.1016/j.palaeo.2006.06.041.

Gómez, J.J., Arias, C., 2010. Rapid warming and ostracods mass extinction at the lower Toarcian (Jurassic) of Central Spain. Mar Micropaleontol 74, 119–135. https://doi.org/10.1016/j.marmicro.2010.02.001.

Gómez, J.J., Goy, A., 2011. Warming-driven mass extinction in the early Toarcian (early Jurassic) of northern and Central Spain. Correlation with other time-equivalent European sections. Palaeogeogr Palaeoclimatol Palaeoecol 306, 176–195. https://doi.org/10.1016/j.palaeo.2011.04.018.

Gómez, J.J., Goy, A., Canales, M.L., 2008. Seawater temperature and carbon isotope variations in belemnites linked to mass extinction during the Toarcian (early Jurassic) in Central and Northern Spain. Comparison with other European sections. Palaeogeogr Palaeoclimatol Palaeoecol 258, 28–58. https://doi.org/10.1016/j.palaeo.2007.11.005.

Gómez, J.J., Comas-Rengifo, M.J., Goy, A., 2016a. The hydrocarbon source rocks of the Pliensbachian (early Jurassic) in the Asturian Basin (Northern Spain): their relationship with the palaeoclimatic oscillations and gamma-ray response. J. Iber. Geol. 42, 259–273. https://doi.org/10.5209/JIGE.53265.

Gómez, J.J., Comas-Rengifo, M.J., Goy, A., 2016b. Palaeoclimatic oscillations in the Pliensbachian (early Jurassic) of the Asturian Basin (Northern Spain). Clim. Past 12, 1199–1214. https://doi.org/10.5194/cp-12-1199-2016.

Gómez, J.J., Sandoval, J., Aguado, R., O'Dogherty, L., Osete, M.L., 2019. The Alpine Cycle in Eastern Iberia: Microplate Units and Geodynamic Stages, pp. 15–27. https://doi.org/10.1007/978-3-030-11295-0_2.

Hesselbo, S.P., Gröcke, D.R., Jenkyns, H.C., Bjerrum, C.J., Farrimond, P., Morgans Bell, H.S., Green, O.R., 2000. Massive dissociation of gas hydrate during a Jurassic oceanic anoxic event. Nature 406, 392–395. https://doi.org/10.1038/35019044.

Hesselbo, S.P., Jenkyns, H.C., Duarte, L.V., Oliveira, L.C.V., 2007. Carbon-isotope record of the early Jurassic (Toarcian) Oceanic Anoxic Event from fossil wood and marine carbonate (Lusitanian Basin, Portugal). Earth Planet. Sci. Lett. 253, 455–470. https://doi.org/10.1016/j.epsl.2006.11.009.

Hesselbo, S.P., Ogg, J.G., Ruhl, M., Hinnov, L.A., Huang, C.J., 2020. The Jurassic Period. In: Gradstein, F.M., Ogg, James G., Schmitz, M.D., Ogg, G.M. (Eds.), Geologic Time Scale 2020, vol. 2. Elsevier, pp. 955–1021. https://doi.org/10.1016/B978-0-12-824360-2.00026-7.

Hoffmann, R., Stevens, K., 2020. The palaeobiology of belemnites – foundation for the interpretation of rostrum geochemistry. Biol. Rev. 95, 94–123. https://doi.org/10.1111/brv.12557.

Ikeda, Y., Arai, N., Sakamoto, W., Yoshida, K., 1999. Trace elements in cephalopod calcified tissue: cuttlebone as a possible tracer for life historical events of cuttlefish. Int. J. PIXE 09, 335–343. https://doi.org/10.1142/S0129083599000437.

Immenhauser, A., Schöne, B.R., Hoffmann, R., Niedermayr, A., 2016. Mollusc and brachiopod skeletal hard parts: Intricate archives of their marine environment. Sedimentology 63, 1–59. https://doi.org/10.1111/sed.12231.

Jenkyns, H.C., 1988. The early Toarcian (Jurassic) anoxic event; stratigraphic, sedimentary and geochemical evidence. Am. J. Sci. 288, 101–151. https://doi.org/10.1126/science.3.53.32.

Jenkyns, H.C., 2010. Geochemistry of oceanic anoxic events. Geochem. Geophys. Geosyst. 11, 1–30. https://doi.org/10.1029/2009GC002788.

Jenkyns, H.C., Jones, C., Gröcke, D., Hesselbo, S., Parkinson, D., 2002. Chemostratigraphy of the Jurassic System: applications, limitations and implications for palaeoceanography. J. Geol. Soc. Lond. 159, 351–378. https://doi.org/10.1144/0016-764901-130.

Jensen, L.T., Morton, P., Twining, B.S., Heller, M.I., Hatta, M., Measures, C.I., John, S., Zhang, R., Pinedo-Gonzalez, P., Sherrell, R.M., Fitzsimmons, J.N., 2020. A comparison of marine Fe and Mn cycling: U.S. GEOTRACES GN01 Western Arctic case study. Geochim. Cosmochim. Acta 288, 138–160. https://doi.org/10.1016/j.gca.2020.08.006.

Korte, C., Hesselbo, S.P., 2011. Shallow marine carbon and oxygen isotope and elemental records indicate icehouse-greenhouse cycles during the early Jurassic. Paleoceanography 26, 1–18. https://doi.org/10.1029/2011PA002160.

Kovács, E.B., Ruhl, M., Silva, R.L., McElwain, J.C., Reolid, M., Korte, C., Ruebsam, W., Hesselbo, S.P., 2024. Mercury sequestration pathways under varying depositional conditions during early Jurassic (Pliensbachian and Toarcian) Karoo-Ferrar volcanism. Palaeogeogr Palaeoclimatol Palaeoecol 637, 111977. https://doi.org/10.1016/j.palaeo.2023.111977.

Krencker, F.-N., Lindström, S., Bodin, S., 2019. A major sea-level drop briefly precedes the Toarcian oceanic anoxic event: implication for early Jurassic climate and carbon cycle. Sci. Rep. 9, 12518. https://doi.org/10.1038/s41598-019-48956-x.

Lepvrier, C., Martínez-García, E., 1990. Fault development and stress evolution of the post-Hercynian Asturian Basin (Asturias and Cantabria, northwestern Spain). Tectonophysics 184, 345–356. https://doi.org/10.1016/0040-1951(90)90447-G.
Li, Q., McArthur, J.M., Atkinson, T.C., 2012. Lower Jurassic belemnites as indicators of palaeo-temperature. Palaeogeogr Palaeoclimatol Palaeoecol 315–316, 38–45. https://doi.org/10.1016/j.palaeo.2011.11.006.
Li, Q., McArthur, J.M., Doyle, P., Janssen, N., Leng, M.J., Müller, W., Reboulet, S., 2013. Evaluating Mg/ca in belemnite calcite as a palaeo-proxy. Palaeogeogr Palaeoclimatol Palaeoecol 388, 98–108. https://doi.org/10.1016/j.palaeo.2013.07.030.
Li, Q., McArthur, J.M., Thirlwall, M.F., Turchyn, A.V., Page, K., Bradbury, H.J., Weis, R., Lowry, D., 2021. Testing for ocean acidification during the early Toarcian using δ44/40Ca and δ88/86Sr. Chem. Geol. 574, 120228 https://doi.org/10.1016/j.chemgeo.2021.120228.
Little, C., Benton, M.J., 1995. Early Jurassic mass extinction: a global long-term event. Geology 23, 495–498.
Martindale, R.C., Aberhan, M., 2017. Response of macrobenthic communities to the Toarcian Oceanic Anoxic Event in northeastern Panthalassa (Ya Ha Tinda, Alberta, Canada). Palaeogeogr Palaeoclimatol Palaeoecol 478, 103–120. https://doi.org/10.1016/j.palaeo.2017.01.009.
Mattioli, E., Pittet, B., Young, J.R., Bown, P.R., 2004. Biometric analysis of Pliensbachian-Toarcian (lower Jurassic) coccoliths of the family Biscutaceae: Intra- and interspecific variability versus palaeoenvironmental influence. Mar Micropaleontol 52, 5–27. https://doi.org/10.1016/j.marmicro.2004.04.004.
Mattioli, E., Pittet, B., Petitpierre, L., Mailliot, S., 2009a. Dramatic decrease of pelagic carbonate production by nannoplankton across the early Toarcian anoxic event (T-OAE). Glob Planet Change 65, 134–145. https://doi.org/10.1016/j.gloplacha.2008.10.018.
Mattioli, E., Pittet, B., Petitpierre, L., Mailliot, S., 2009b. Dramatic decrease of pelagic carbonate production by nannoplankton across the early Toarcian anoxic event (T-OAE). Glob Planet Change 65, 134–145. https://doi.org/10.1016/j.gloplacha.2008.10.018.
McArthur, J.M., Donovan, D.T., Thirlwall, M.F., Fouke, B.W., Mattey, D., 2000. Strontium isotope profile of the early Toarcian (Jurassic) oceanic anoxic event, the duration of ammonite biozones, and belemnite palaeotemperatures. Earth Planet. Sci. Lett. 179, 269–285. https://doi.org/10.1016/S0012-821X(00)00111-4.
McArthur, J.M., Doyle, P., Leng, M.J., Reeves, K., Williams, C.T., Garcia-Sanchez, R., Howarth, R.J., 2007. Testing palaeo-environmental proxies in Jurassic belemnites: Mg/Ca, Sr/Ca, Na/Ca, δ18O and δ13C. Palaeogeogr Palaeoclimatol Palaeoecol 252, 464–480. https://doi.org/10.1016/j.palaeo.2007.05.006.
McArthur, J.M., Howarth, R.J., Shields, G.A., Zhou, Y., 2020. Strontium isotope stratigraphy. In: Geologic Time Scale 2020. Elsevier, pp. 211–238. https://doi.org/10.1016/B978-0-12-824360-2.00007-3.
McElwain, J.C., Wade-Murphy, J., Hesselbo, S.P., 2005. Changes in carbon dioxide during an oceanic anoxic event linked to intrusion into Gondwana coals. Nature 435, 479–482. https://doi.org/10.1038/nature03618.
Müller, T., Price, G.D., Bajnai, D., Nyerges, A., Kesjár, D., Raucsik, B., Varga, A., Judik, K., Fekete, J., May, Z., Pálfy, J., 2016. New multiproxy record of the Jenkyns Event (also known as the Toarcian Oceanic Anoxic Event) from the Mecsek Mountains (Hungary): differences, duration and drivers. Sedimentology 64, 66–86. https://doi.org/10.1111/sed.12332.
Müller, T., Jurikova, H., Gutjahr, M., Tomašových, A., Schlögl, J., Liebetrau, V., Duarte, L., Milovský, R., Suan, G., Mattioli, E., Pittet, B., Eisenhauer, A., 2020. Ocean acidification during the early Toarcian extinction event: evidence from boron isotopes in brachiopods. Geology 48, 1184–1188. https://doi.org/10.1130/G47781.1.
Nätscher, P.S., Dera, G., Reddin, C.J., Rita, P., De Baets, K., 2021. Morphological response accompanying size reduction of belemnites during an Early Jurassic hyperthermal event modulated by life history. Sci. Rep. 11, 14480. https://doi.org/10.1038/s41598-021-93850-0.
Neige, P., Weis, R., Fara, E., 2021. Ups and downs of belemnite diversity in the Early Jurassic of Western Tethys. Palaeontology 64, 263–283. https://doi.org/10.1111/pala.12522.
Page, K.N., 2003. The lower Jurassic of Europe: its subdivision and correlation. Geological Survey of Denmark and Greenland Bulletin 1, 23–59.
Pálfy, J., Smith, P.L., 2000. Synchrony between Early Jurassic extinction, oceanic anoxic event, and the Karoo-Ferrar flood basalt volcanism. Geology 28, 747–750. https://doi.org/10.1130/0091-7613(2000)028<0747:SBEJEO>2.3.CO;2.
Percival, L.M.E., Witt, M.L.I., Mather, T.A., Hermoso, M., Jenkyns, H.C., Hesselbo, S.P., Al-Suwaidi, A.H., Storm, M.S., Xu, W., Ruhl, M., 2015. Globally enhanced mercury deposition during the end-Pliensbachian extinction and Toarcian OAE: a link to the Karoo-Ferrar Large Igneous Province. Earth Planet. Sci. Lett. 428, 267–280. https://doi.org/10.1016/j.epsl.2015.06.064.
Percival, L.M.E., Cohen, A.S., Davies, M.K., Dickson, A.J., Hesselbo, S.P., Jenkyns, H.C., Leng, M.J., Mather, T.A., Storm, M.S., Xu, W., 2016. Osmium isotope evidence for two pulses of increased continental weathering linked to Early Jurassic volcanism and climate change. Geology 44, 759–762. https://doi.org/10.1130/G37997.1.
Peti, L., Thibault, N., 2017. Abundance and size changes in the calcareous nannofossil Schizosphaerella – Relation to sea-level, the carbonate factory and palaeoenvironmental change from the Sinemurian to earliest Toarcian of the Paris Basin. Palaeogeogr Palaeoclimatol Palaeoecol 485, 271–282. https://doi.org/10.1016/j.palaeo.2017.06.019.
Piazza, V., Duarte, L.V., Renaudie, J., Aberhan, M., 2019. Reductions in body size of benthic macroinvertebrates as a precursor of the early Toarcian (Early Jurassic) extinction event in the Lusitanian Basin, Portugal. Paleobiology 45, 296–316. https://doi.org/10.1017/pab.2019.11.
Pittet, B., Suan, G., Lenoir, F., Duarte, L.V., Mattioli, E., 2014. Carbon isotope evidence for sedimentary discontinuities in the lower Toarcian of the Lusitanian Basin (Portugal): Sea level change at the onset of the Oceanic Anoxic Event. Sediment Geol 303, 1–14. https://doi.org/10.1016/j.sedgeo.2014.01.001.
Poehle, S., Koschinsky, A., 2017. Depth distribution of Zr and Nb in seawater: the potential role of colloids or organic complexation to explain non-scavenging-type behavior. Mar. Chem. 188, 18–32. https://doi.org/10.1016/j.marchem.2016.12.001.
Price, G., 1999. The evidence and implications of polar ice during the Mesozoic. Earth Sci. Rev. 48, 183–210. https://doi.org/10.1016/S0012-8252(99)00048-3.
Quintana, L., Pulgar, J.A., Alonso, J.L., 2015. Displacement transfer from borders to interior of a plate: a crustal transect of Iberia. Tectonophysics 663, 378–398. https://doi.org/10.1016/j.tecto.2015.08.046.
Remick, K.A., Helmann, J.D., 2023. The elements of life: A biocentric tour of the periodic table, pp. 1–127. https://doi.org/10.1016/bs.ampbs.2022.11.001.
Reolid, M., Mattioli, E., Duarte, L.V., Marok, A., 2020. The Toarcian Oceanic Anoxic Event and the Jenkyns Event (IGCP-655 final report). Episodes 43, 833–844. https://doi.org/10.18814/epiiugs/2020/020051.
Rita, P., De Baets, K., Schlott, M., 2018. Rostrum size differences between Toarcian belemnite battlefields. Fossil Record 21, 171–182. https://doi.org/10.5194/fr-21-171-2018.
Rita, P., Nätscher, P., Duarte, L.V., Weis, R., De Baets, K., 2019. Mechanisms and drivers of belemnite body-size dynamics across the Pliensbachian–Toarcian crisis. R. Soc. Open Sci. 6, 190494 https://doi.org/10.1098/rsos.190494.
Rita, P., Weis, R., Duarte, L.V., De Baets, K., 2021. Taxonomical diversity and palaeobiogeographical affinity of belemnites from the Pliensbachian–Toarcian <scp>GSSP</scp> (Lusitanian Basin, Portugal). Pap Palaeontol 7, 1321–1349. https://doi.org/10.1002/spp2.1343.
Rocha, R.B., Mattioli, E., Duarte, L.V., Pittet, B., Elmi, S., Mouterde, R., Cabral, M.C., Comas-Rengifo, M.J., Gómez, J.J., Goy, A., Hesselbo, S.P., Jenkyns, H.C., Littler, K., Mailliot, S., Oliveira, L.C.V., Osete, M.L., Perilli, N., Pinto, S., Ruget, C., Suan, G., 2016. Base of the Toarcian Stage of the Lower Jurassic defined by the Global Boundary Stratotype Section and Point (GSSP) at the Peniche section (Portugal). Episodes 39, 460–481. https://doi.org/10.18814/epiiugs/2016/v39i3/99741.
Rodrigues, B., Duarte, L.V., Mendonça Filho, J.G., Santos, L.G., Donizeti de Oliveira, A., 2016. Evidence of terrestrial organic matter deposition across the early Toarcian recorded in the northern Lusitanian Basin, Portugal. Int. J. Coal Geol. 168, 35–45. https://doi.org/10.1016/j.coal.2016.06.016.
Rodrigues, B., Silva, R.L., Reolid, M., Mendonça Filho, J.G., Duarte, L.V., 2019. Sedimentary organic matter and δ13CKerogen variation on the southern Iberian palaeomargin (Betic Cordillera, SE Spain) during the latest Pliensbachian–Early Toarcian. Palaeogeogr Palaeoclimatol Palaeoecol 534, 109342. https://doi.org/10.1016/j.palaeo.2019.109342.
Rodrigues, B., Duarte, L.V., Silva, R.L., Mendonça Filho, J.G., 2020a. Sedimentary organic matter and early Toarcian environmental changes in the Lusitanian Basin (Portugal). Palaeogeogr Palaeoclimatol Palaeoecol 554, 109781. https://doi.org/10.1016/j.palaeo.2020.109781.
Rodrigues, B., Silva, R.L., Filho, J.G.M., Sadki, D., Mendonça, J.O., Duarte, L.V., 2020b. Late Pliensbachian–Early Toarcian palaeoenvironmental dynamics and the Pliensbachian–Toarcian Event in the Middle Atlas Basin (Morocco). Int. J. Coal Geol. 217, 103339 https://doi.org/10.1016/j.coal.2019.103339.
Rodrigues, B., Silva, R.L., Mendonça Filho, J.G., Comas-Rengifo, M.J., Goy, A., Duarte, L. V., 2020c. Kerogen assemblages and δ13CKerogen of the uppermost Pliensbachian–lower Toarcian succession of the Asturian Basin (northern Spain). Int. J. Coal Geol. 229, 103573 https://doi.org/10.1016/j.coal.2020.103573.
Rodrigues, B., Silva, R.L., Mendonça Filho, J.G., Reolid, M., Sadki, D., Comas-Rengifo, M. J., Goy, A., Duarte, L.V., 2021. The Phytoclast Group as a tracer of palaeoenvironmental changes in the early Toarcian. Geol. Soc. Lond. Spec. Publ. 514, 291–307. https://doi.org/10.1144/SP514-2020-271.
Rosales, I., Quesada, S., Robles, S., 2001. Primary and diagenetic isotopic signals in fossils and hemipelagic carbonates: the Lower Jurassic of northern Spain. Sedimentology 48, 1149–1169. https://doi.org/10.1046/j.1365-3091.2001.00412.x.
Rosales, I., Quesada, S., Robles, S., 2004a. Paleotemperature variations of Early Jurassic seawater recorded in geochemical trends of belemnites from the Basque-Cantabrian basin, northern Spain. Palaeogeogr Palaeoclimatol Palaeoecol 203, 253–275. https://doi.org/10.1016/S0031-0182(03)00686-2.
Rosales, I., Robles, S., Quesada, S., 2004b. Elemental and Oxygen Isotope Composition of Early Jurassic Belemnites: Salinity vs. Temperature Signals. J. Sediment. Res. 74, 342–354. https://doi.org/10.1306/112603740342.
Ruebsam, W., Mayer, B., Schwark, L., 2019. Cryosphere carbon dynamics control early Toarcian global warming and sea level evolution. Glob Planet Change 172, 440–453. https://doi.org/10.1016/j.gloplacha.2018.11.003.
Ruebsam, W., Reolid, M., Sabatino, N., Masetti, D., Schwark, L., 2020a. Molecular paleothermometry of the early Toarcian climate perturbation. Glob Planet Change 195, 103351. https://doi.org/10.1016/j.gloplacha.2020.103351.
Ruebsam, W., Thibault, N., Al-Husseini, M., 2020b. Early Toarcian glacio-eustatic unconformities and chemostratigraphic black holes. In: Montenari, M. (Ed.), Stratigraphy & Timescales. Academic Press, pp. 629–676. https://doi.org/10.1016/bs.sats.2020.08.006.
Ruhl, M., Hesselbo, S.P., Hinnov, L., Jenkyns, H.C., Xu, W., Riding, J.B., Storm, M., Minisini, D., Ullmann, C.V., Leng, M.J., 2016. Astronomical constraints on the duration of the early Jurassic Pliensbachian Stage and global climatic fluctuations. Earth Planet. Sci. Lett. 455, 149–165. https://doi.org/10.1016/j.epsl.2016.08.038.
Ruhl, M., Hesselbo, S.P., Jenkyns, H.C., Xu, W., Silva, R.L., Matthews, K.J., Mather, T.A., Mac Niocaill, C., Riding, J.B., 2022. Reduced plate motion controlled timing of Early

Jurassic Karoo-Ferrar large igneous province volcanism. Sci. Adv. 8 https://doi.org/10.1126/sciadv.abo0866.
Silva, R.L., Duarte, L.V., 2015. Organic matter production and preservation in the Lusitanian Basin (Portugal) and Pliensbachian climatic hot snaps. Glob Planet Change 131, 24–34. https://doi.org/10.1016/j.gloplacha.2015.05.002.
Silva, R.L., Duarte, L.V., Wach, G.D., Ruhl, M., Sadki, D., Gómez, J.J., Hesselbo, S.P., Xu, W., O'Connor, D., Rodrigues, B., Filho, J.G.M., 2021a. An Early Jurassic (Sinemurian–Toarcian) stratigraphic framework for the occurrence of Organic Matter Preservation Intervals (OMPIs). Earth Sci Rev 221, 103780. https://doi.org/10.1016/j.earscirev.2021.103780.
Silva, R.L., Ruhl, M., Barry, C., Reolid, M., Ruebsam, W., 2021b. Pacing of late Pliensbachian and early Toarcian carbon cycle perturbations and environmental change in the westernmost Tethys (La Cerradura Section, Subbetic zone of the Betic Cordillera, Spain). Geol. Soc. Lond. Spec. Publ. 514, 387–408. https://doi.org/10.1144/SP514-2021-27.
Slater, S.M., Twitchett, R.J., Danise, S., Vajda, V., 2019. Substantial vegetation response to Early Jurassic global warming with impacts on oceanic anoxia. Nat. Geosci. https://doi.org/10.1038/s41561-019-0349-z.
Storm, M.S., Hesselbo, S.P., Jenkyns, H.C., Ruhl, M., Ullmann, C.V., Xu, W., Leng, M.J., Riding, J.B., Gorbanenko, O., 2020. Orbital pacing and secular evolution of the Early Jurassic carbon cycle. Proc. Natl. Acad. Sci. 117, 3974–3982. https://doi.org/10.1073/pnas.1912094117.
Suan, G., Mattioli, E., Pittet, B., Mailliot, S., Lécuyer, C., 2008. Evidence for major environmental perturbation prior to and during the Toarcian (Early Jurassic) oceanic anoxic event from the Lusitanian Basin, Portugal. Paleoceanography 23, 1–14. https://doi.org/10.1029/2007PA001459.
Suan, G., Mattioli, E., Pittet, B., Lécuyer, C., Suchéras-Marx, B., Duarte, L.V., Philippe, M., Reggiani, L., Martineau, F., 2010. Secular environmental precursors to Early Toarcian (Jurassic) extreme climate changes. Earth Planet. Sci. Lett. 290, 448–458. https://doi.org/10.1016/j.epsl.2009.12.047.
Suárez Vega, L.C., 1974. Estratigrafía del jurásico en Asturias (PhD thesis). C.S.I.C, Madrid.
Them, T.R., Gill, B.C., Caruthers, A.H., Gröcke, D.R., Tulsky, E.T., Martindale, R.C., Poulton, T.P., Smith, P.L., 2017. High-resolution carbon isotope records of the Toarcian Oceanic Anoxic Event (Early Jurassic) from North America and implications for the global drivers of the Toarcian carbon cycle. Earth Planet. Sci. Lett. 459, 118–126. https://doi.org/10.1016/j.epsl.2016.11.021.
Them, T.R., Gill, B.C., Caruthers, A.H., Gerhardt, A.M., Gröcke, D.R., Lyons, T.W., Marroquín, S.M., Nielsen, S.G., Trabucho Alexandre, J.P., Owens, J.D., 2018. Thallium isotopes reveal protracted anoxia during the Toarcian (Early Jurassic) associated with volcanism, carbon burial, and mass extinction. Proc. Natl. Acad. Sci. 115, 6596–6601. https://doi.org/10.1073/pnas.1803478115.
Them, T.R., Jagoe, C.H., Caruthers, A.H., Gill, B.C., Grasby, S.E., Gröcke, D.R., Yin, R., Owens, J.D., 2019. Terrestrial sources as the primary delivery mechanism of mercury to the oceans across the Toarcian Oceanic Anoxic Event (Early Jurassic). Earth Planet. Sci. Lett. 507, 62–72. https://doi.org/10.1016/j.epsl.2018.11.029.
Thibault, N., Ruhl, M., Ullmann, C.V., Korte, C., Kemp, D.B., Gröcke, D.R., Hesselbo, S.P., 2018. The wider context of the Lower Jurassic Toarcian oceanic anoxic event in Yorkshire coastal outcrops, UK. Proc. Geol. Assoc. 129, 372–391. https://doi.org/10.1016/j.pgeola.2017.10.007.
Tribovillard, N., Algeo, T.J., Lyons, T., Riboulleau, A., 2006. Trace metals as paleoredox and paleoproductivity proxies: an update. Chem. Geol. 232, 12–32. https://doi.org/10.1016/j.chemgeo.2006.02.012.
Tribovillard, N., Algeo, T.J., Baudin, F., Riboulleau, A., 2012. Analysis of marine environmental conditions based onmolybdenum–uranium covariation—applications to Mesozoic paleoceanography. Chem. Geol. 324–325, 46–58. https://doi.org/10.1016/j.chemgeo.2011.09.009.
Trujillo, A., Thurman, H., 2017. Essentials of Oceanography. Pearson.
Turan, C., Yaglioglu, D., 2010. Population identification of common cuttlefish (Sepia officinalis) inferred from genetic, morphometric and cuttlebone chemistry data in the NE Mediterranean Sea. Sci. Mar. 74, 77–86. https://doi.org/10.3989/scimar.2010.74n107.
Ullmann, C.V., Korte, C., 2015. Diagenetic alteration in low-Mg calcite from macrofossils: a review. Geological Quarterly. https://doi.org/10.7306/gq.1217.
Ullmann, C.V., Pogge von Strandmann, P.A.E., 2017. The effect of shell secretion rate on Mg/Ca and Sr/Ca ratios in biogenic calcite as observed in a belemnite rostrum. Biogeosciences 14, 89–97. https://doi.org/10.5194/bg-14-89-2017.
Ullmann, C.V., Hesselbo, Stephen P., Korte, C., 2013. Tectonic forcing of early to middle jurassic seawater Sr/Ca. Geology 41, 1211–1214. https://doi.org/10.1130/G34817.1.
Ullmann, C.V., Thibault, N., Ruhl, M., Hesselbo, S.P., Korte, C., 2014. Effect of a Jurassic oceanic anoxic event on belemnite ecology and evolution. Proc. Natl. Acad. Sci. 111, 10073–10076. https://doi.org/10.1073/pnas.1320156111.
Ullmann, C.V., Frei, R., Korte, C., Hesselbo, S.P., 2015. Chemical and isotopic architecture of the belemnite rostrum. Geochim. Cosmochim. Acta 159, 231–243. https://doi.org/10.1016/j.gca.2015.03.034.
Ullmann, C.V., Boyle, R., Duarte, L.V., Hesselbo, S.P., Kasemann, S.A., Klein, T., Lenton, T.M., Piazza, V., Aberhan, M., 2020. Warm afterglow from the Toarcian Oceanic Anoxic Event drives the success of deep-adapted brachiopods. Sci. Rep. 10, 6549. https://doi.org/10.1038/s41598-020-63487-6.
Valenzuela, M., 1988. Estratigrafía, sedimentología y paleogeografía del Jurásico de Asturias. PhD thesis. Universidad Oviedo.
Valenzuela, M., García-Ramos, J.C., Suárez De Centi, C., 1986. The Jurassic sedimentation in Asturias (N Spain). Trabajos De Geología 16, 121–133.
van de Schootbrugge, B., McArthur, J.M., Bailey, T.R., Rosenthal, Y., Wright, J.D., Miller, K.G., 2005. Toarcian oceanic anoxic event: an assessment of global causes using belemnite C isotope records. Paleoceanography 20, PA3008. https://doi.org/10.1029/2004PA001102.
Wierzbowski, H., Joachimski, M.M., 2007. Stable isotopes, elemental distribution, and growth rings of belemnopsid belemnite rostra: Proxies for belemnite life habitat. Palaios 24, 377–386. https://doi.org/10.2110/palo.2008.p08-101r.
Wignall, P.B., Newton, R.J., Little, C.T.S., 2005. The timing of paleoenvironmental changes and cause-and-effect relationships during the early Jurassic mass extinction in Europe. Am. J. Sci. 305, 1014–1032.
Xu, W., Ruhl, M., Jenkyns, H.C., Leng, M.J., Huggett, J.M., Minisini, D., Ullmann, C.V., Riding, J.B., Weijers, J.W.H., Storm, M.S., Percival, L.M.E., Tosca, N.J., Idiz, E.F., Tegelaar, E.W., Hesselbo, S.P., 2018. Evolution of the Toarcian (Early Jurassic) carbon-cycle and global climatic controls on local sedimentary processes (Cardigan Bay Basin, UK). Earth Planet. Sci. Lett. 484, 396–411. https://doi.org/10.1016/j.epsl.2017.12.037.
Zheng, X.-Y., Beard, B.L., Neuman, M., Fahnestock, M.F., Bryce, J.G., Johnson, C.M., 2022. Stable potassium (K) isotope characteristics at mid-ocean ridge hydrothermal vents and its implications for the global K cycle. Earth Planet. Sci. Lett. 593, 117653 https://doi.org/10.1016/j.epsl.2022.117653.
Zumholz, K., Hansteen, T.H., Klügel, A., Piatkowski, U., 2006. Food effects on statolith composition of the common cuttlefish (Sepia officinalis). Mar. Biol. 150, 237–244. https://doi.org/10.1007/s00227-006-0342-0.